Computed tomographic findings in a suspected disseminated primitive neuroectodermal tumour in a young dog

Frances M*[a], Lester NV[a], Lenard ZM[a], Nicholls PK[b]
*Corresponding author
[a]Veterinary Imaging Centre, 305 Selby Street North Osborne Park, Western Australia 6017, Australia; mfrancesvet@gmail.com
[b]School of Veterinary and Life Sciences, Murdoch University, Murdoch, Western Australia 6150, Australia

ABSTRACT

A two and a half-year-old American Staffordshire bull terrier was presented with seizures, unilateral blindness consistent with a lesion at the level of the optic nerve and bilateral hindleg ataxia progressing to paresis. Computed tomography (CT) of the brain and spine identified a mineralised suprasellar mass which extended along both optic nerves. The dog recovered uneventfully from anaesthesia but died within 24 hours. Necropsy and histopathology confirmed the CT findings, identifying neoplastic invasion of the cerebrum and brainstem with extensive meningeal dissemination involving the entire spinal cord. Histologic features and immunohistochemical staining were most consistent with a primitive neuroectodermal tumour, although some typical features, such as cellular pseudorosettes, were not found. The difficulty in forming a definitive conclusion in this case is consistent with previous reports of other juvenile central nervous system tumours in which the presence of multiple cell types within the mass and conflicting immunohistochemical characteristics are confounding factors. This case highlights the clinical utility of computed tomography in characterising intracranial mass lesions in young dogs presenting with seizures and multifocal central neurologic abnormalities. Neoplasia resulting in these clinical and imaging findings in young dogs is commonly aggressive in nature and should be included as a differential diagnosis.
Aust Vet Pract 2013;43(4):521-526

A two and a half-year-old male neutered American Staffordshire bull terrier weighing 33 kg was examined by a specialist in neurology after referral from a general practitioner. The dog had a three month history of seizures and multifocal central neurologic deficits. Initially the dog was presented for acute onset of generalized seizures over a period of two days. One week later, the dog developed exophthalmos of the right globe with chemosis and unilateral right sided blindness. Neuroanatomic localisation within the visual pathway was consistent with an optic nerve lesion. Analysis of cerebrospinal fluid collected by cisternal puncture indicated elevated protein concentration (138 mg/dL, reference range <30 mg/dL). A mixed cell population was present (neutrophils 4%, lymphocytes 29.8%, large mononuclear cells 65.7%, eosinophils 0.5%) indicating the lack of an inflammatory response. Serologic testing was negative for *Cryptococcus sp.* and *Neospora sp.* Toxoplasma titres were consistent with prior exposure and possible latent infection (IgG IFAT 1:256, IgM IFAT <1:32). At the onset of blindness and exophthalmos, the dog was treated empirically with prednisolone at 10 mg twice daily. The dose was tapered over three weeks and was then discontinued. Trimethoprim/sulphadiazine was also administered at this time at 480 mg twice daily for 10 days. The exophthalmos resolved but the unilateral visual deficits persisted. The dog had a further cluster of seizures at which time phenobarbitone was administered at 75 mg twice daily, increasing to 100 mg twice daily after the serum phenobarbitone concentration was measured at 17.9 mg/L. No further seizures were observed, however the dog developed bilateral hindleg ataxia which progressed to paresis over a period of three to four weeks. Re- treatment with prednisolone (20 mg twice daily) and trimethoprim sulfur (480 mg twice daily) had no effect on the ataxia. The dog was then referred to the Veterinary Imaging Centre by the neurologist for imaging of the brain and spinal cord.

Computed tomographic imaging of the head and spine (Brilliance 6 Phillips Healthcare) was performed before and one minute after intravenous administration of non-ionic iodinated contrast medium (600mg/kg, Ioversol, Mallinckrodt). Additional scans were performed on the entire spine after a five minute delay. Images were examined in bone, soft tissue and brain windows using multiplanar reformats.

Imaging findings included moderate ventriculomegaly of the lateral, third and fourth ventricles with relatively symmetric dilation of the lateral ventricles. On pre-contrast images in the midline suprasellar region, a 15 x 15 x 12 mm poorly marginated region of amorphous mineralisation (300HU) was identified that extended caudally in the region of the hypothalamus and rostrally in association with the optic chiasm (Figure 1A). The mineralisation also extended from the optic chiasm along the path of both optic nerves over a distance of 15 mm within the optic canal. The post-contrast CT images showed mild enhancement of the mass, extending rostrally within both sides of the ventral aspect of the frontal lobe toward the olfactory lobe. This created a mass effect (Figures 1B and 1C).

Figure 1A. Computed tomographic image in the transverse plane of a two and a half-year-old American Staffordshire bull terrier with clinical signs consistent with multianatomic central nervous system disease. There is a mineralised suprasellar mass (arrows). Bone window, pre-contrast.

Figure 1B. Computed tomographic image in the transverse plane of a two and a half-year-old American Staffordshire bull terrier with clinical signs consistent with multianatomic central nervous system disease. There is a mineralised suprasellar mass (arrow) with mild ventriculomegaly (arrowhead). Mild contrast enhancement was noted within the mass. Soft tissue window, one minute post–contrast.

The optic nerves were thickened and measured 4.4 mm diameter (left) and 6mm (right). They were hypo-attenuating and displayed moderate meningeal enhancement. At the level of the right globe, the right optic nerve was irregularly marginated with a bulbous expansion of the nerve to a diameter of 10 mm with moderate patchy parenchymal enhancement (Figure 1D). No spinal cord abnormalities were identified. Based on the CT findings, the prioritised differential diagnoses were an optic pathway glioma, craniopharyngioma, germ cell tumour, or lymphoma.

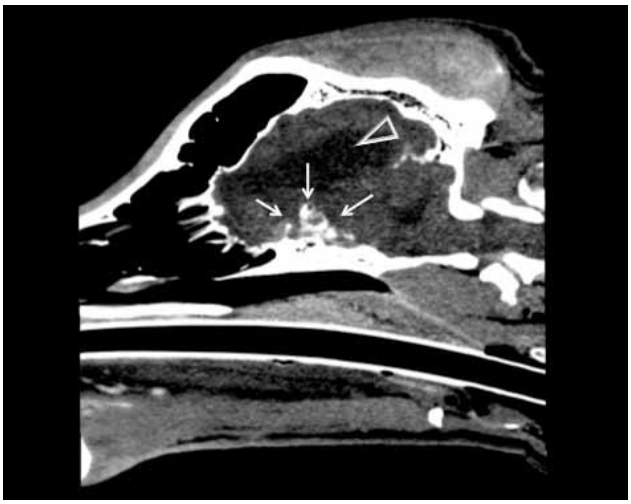

Figure 1C. Computed tomographic image in the sagittal plane of a two and a half-year-old American Staffordshire bull terrier with clinical signs consistent with multianatomic central nervous system disease. There is a mineralised suprasellar mass (arrows) and mild ventriculomegaly (open arrowhead). Soft tissue window, post -contrast administration, rostral is to the left.

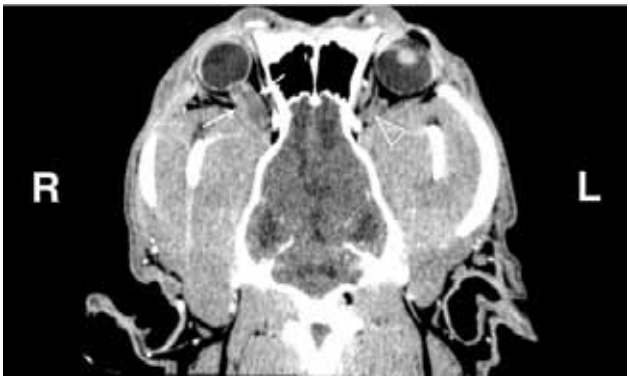

Figure 1D. Computed tomographic image in the oblique dorsal plane of a two and a half year-old American Staffordshire bull terrier with clinical signs consistent with multianatomic central nervous system disease. There is marked thickening of the right optic nerve (arrows). The origin of the left optic nerve can be seen in the retrobulbar space (arrowhead), however it is not continuous with the left globe in this plane. Soft tissue window, post-contrast administration.

The dog recovered from anaesthesia uneventfully with no deterioration in its neurologic status noted, but was found dead at home approximately 24 hours later. Necropsy was performed 18 hours later but a definitive cause of death was not identified.

Necropsy revealed a non-encapsulated, tan, 17 x 15 mm mass on the ventral aspect of the brain rostral to the optic chiasm, compressing the adjacent brain tissue (Figure 2). The mass was soft with foci of gritty mineralisation noted when cut. It extended superficially along the external surface of the brain and both optic nerves. The maximal diameter of optic nerve was 9 mm (right) and 6 mm (left). Caudal extension of the mass continued over the pituitary gland and the pons, forming a poorly defined, plaque-like tan mass 15 mm in diameter which obscured the surface features of the underlying brain. Serial slicing of the formalin fixed brain

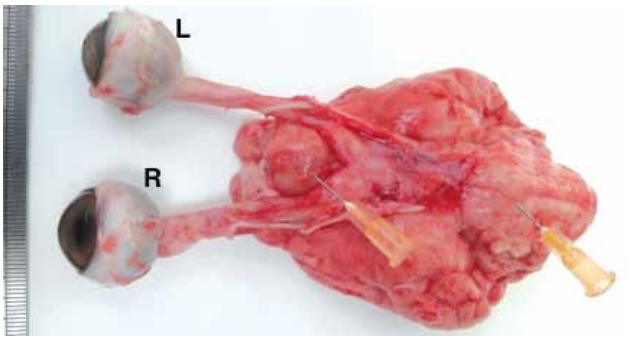

Figure 2. Gross pathologic image of the ventral aspect of brain from a two and a half year-old American Staffordshire bull terrier with clinical signs consistent with multianatomic central nervous system disease. There is a mass rostral to optic chiasm (left needle) and extension over the pons (right needle), with thickened left and right optic nerves.

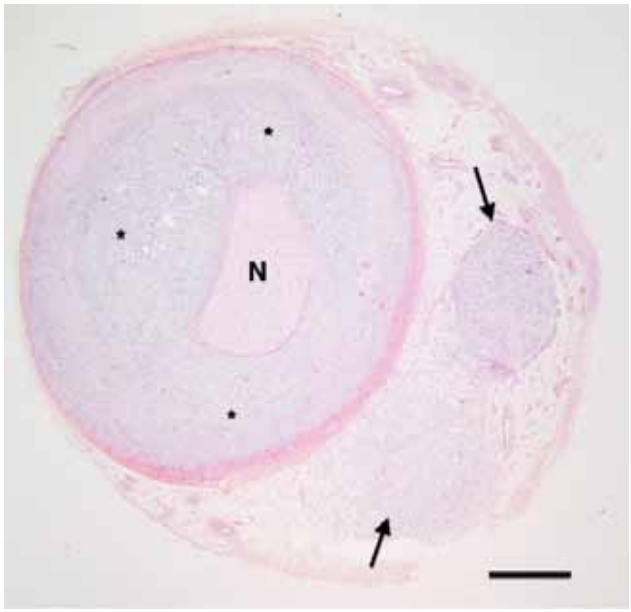

Figure 3A. Photomicrograph of a section through a tumour involving the right optic nerve of a two and a half year-old American Staffordshire bull terrier. The nerve (N) is surrounded by a densely cellular neoplastic infiltrate (*), with invasion in the surrounding adipose and loose fibrovascular connective tissues (arrows). Haematoxylin and eosin. Magnification x1.25, Bar = 1 mm

revealed thickened meninges extending from the rostral aspect of the mass laterally along both optic nerves, ventrally in the region of the pons and dorsolaterally around the midbrain. Serial slicing of the formalin fixed spinal cord showed filling of the subdural space by tan tissue that enveloped the nerve roots. This extended along the cervical spinal cord, through the thoracic segments to the lumbar and sacral spinal cord.

Samples were examined under light microscopy after haematoxylin and eosin staining. Sections from the mass and meninges showed a poorly demarcated, densely cellular infiltrate that in places extended into the adjacent brain, most notably in the rostral cerebrum. There was extension into surrounding connective tissues of the optic nerve, around the spinal cord and nerve roots and dorsolaterally around midbrain and pons,

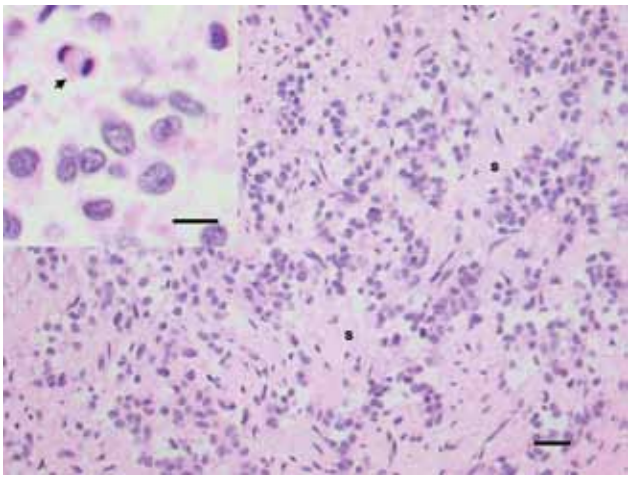

Figure 3B. Photomicrograph of a section of the tumour from a two and a half-year-old American Staffordshire bull terrier. Tumour cells are clustered into packets by a fibrillar stroma (s). Haematoxylin and eosin, magnification x40 Bar = 20µm. **Insert:** cells have round to oval nucleus and poorly defined cytoplasm. Note the mitotic figure (arrow head). Haematoxylin and eosin, x100 oil immersion, Bar = 10µm

and over the dorsal wall of the fourth ventricle (Figure 3A). Occasional foci of mineralisation and metaplastic bone formation were noted. The mass comprised randomly-oriented, parallel arrays of spindle-shaped cells, with a pale, elongated oval nucleus, finely stippled chromatin, and eosinophilic cytoplasmic processes having an indistinct outline. Elsewhere, the cells had a round nucleus and scant cytoplasm, and formed a solid sheet, with frequent mitoses and multifocal areas of necrosis, or a more packeted arrangement amongst a spindle cell stroma (Figure 3B).

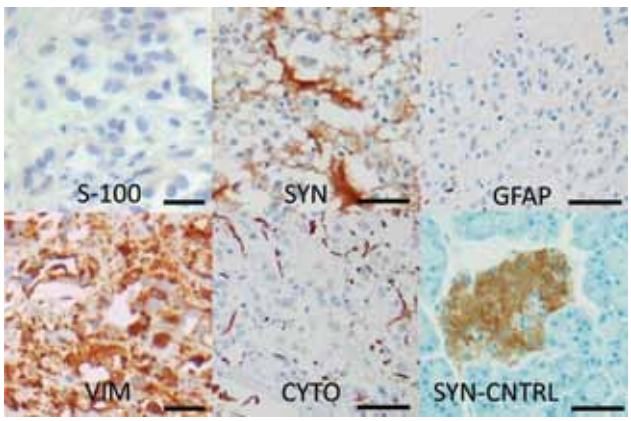

Figure 3C. Immunohistochemical findings. S-100 immunohistochemistry was negative, bar = 20 µm. SYN (synaptophysin) showed moderate positive immunoreactivity, bar = 50 µm. GFAP (glial fibrillary acidic protein) immunohistochemistry was negative (note the packeted arrangements of the cells), bar = 50 µm. VIM (vimentin) showed strong immunoreactivity, bar = 20 µm. CYTO (cytokeratin) was negative except for occasional fibrillar processes, bar = 50 µm. SYN-CNTRL (synaptophysin, positive control: Islet of Langerhans reacted positively amongst surrounding negative exocrine pancreas), Bar = 50 µm

Immunohistochemistry showed no significant immunoreactivity for S-100 or glial fibrillary acidic protein (GFAP), with occasional cytokeratin-positive fibrillar processes, and widespread vimentin immunoreactivity. Synaptophysin demonstrated moderate immunoreactivity in many areas (Figure 3C). Epithelial membrane antigen, although considered useful in identifying tumours of meningeal origin, failed to demonstrate positive control reactions and so was not pursued further. The findings were considered most consistent with a primitive neuroectodermal tumour (PNET).

DISCUSSION

Neoplasia is an uncommon cause of seizures in young adult dogs with infectious and inflammatory disorders or idiopathic epilepsy more likely.[1] Advanced imaging of the central nervous system can play a key role in differentiating these conditions. Computed tomography is a readily available and rapid method of identifying central nervous system pathology, particularly where multifocal signs may make MRI prohibitive due to the duration of anaesthesia required to image several regions. Computed tomography is considered reliable in people for detection of calcification and haemorrhage and is used for assessment in people presenting with acute neurologic signs.[2] In people, MRI has been reported to be superior for detecting brain tumours not identified on CT and may be more sensitive for detection of meningeal dissemination.[2] In this case MRI may have provided greater information than CT regarding the extent of disease and for this reason it is the modality of choice in similar cases at many institutions. The reported findings for many of the differential diagnoses considered in this dog are however non-specific on both MRI and CT, with definitive diagnosis relying on histopathology.[3-8]

The computed tomographic findings in this case were consistent with the location and extent of the intracranial pathology and CT was particularly useful at characterizing mineralisation and optic nerve changes. Involvement of the meninges overlying the spinal cord was not identified. In this dog contrast enhanced imaging of the spinal cord was limited due to the short delay between scans which was necessary to re-plan, and allow for tube cooling. Computed tomography is insensitive for detection of meningeal disease including leptomeningeal metastasis and subtle enhancement may not be appreciated even if images are obtained immediately post intravenous administration of contrast.[9,10] Magnetic resonance imaging is reportedly more sensitive in the detection of meningeal disease, but false negatives may also occur with this modality.[11,12] Differential diagnoses based on the imaging appearance of a mineralised suprasellar mass with optic nerve involvement, and the dog's age, included optic pathway glioma, craniopharyngioma and germ cell tumor.[13-18] Optic pathway gliomas are rare but have been reported in dogs including a three and a half year-old Labrador with thickened optic nerves, and neoplastic tissue extending into the hypothalamus forming a non-mineralised suprasellar mass.[18] Mineralisation within the neoplastic tissue may occur in people with optic pathway gliomas, as does dissemination along CSF pathways. Imaging features of this tumour type are not described in dogs but are poorly predictive of malignancy in people.[19] Both craniopharyngiomas and germ cell tumours arise from neoplastic transformation of embryologic remnants, and although rare, have been reported in young dogs.[20,21] Their growth pattern is unpredictable and classification of these tumours has been described as problematic.[16,21,22] Lymphoma was also a consideration based on the imaging features.[3] The widespread meningeal dissemination identified on microscopic examination led to the addition of oligodendroglioma and meningioangiomatosis to the differential diagnoses, both of which are reported in young dogs and may conform to this anatomic distribution.[4,5,23-26] When considering the histologic interpretation, the negative GFAP reaction eliminated tumours of astrocytic origin, and made tumours of other glial origin unlikely.[27] Ependymal and choroid plexus tumours typically have rosettes and an overt epithelial appearance respectively, which were not evident.[28] The cysts, tubules and extensive squamous differentiation of craniopharyngiomas were absent, and the microscopic features and positive synaptophysin immunohistochemistry did not support a tumour of meningeal origin. Germ cell tumours typically express cytokeratin in a strong and widespread pattern unlike that seen in this dog, and often have hepatoid cells, glandular formations and squamous differentiation.[29,30] The positive synaptophysin reaction was consistent with a neuronal or embryonal origin.[28] Neuronal tumours such as olfactory neuroblastoma typically originate in the upper nasal cavity and mostly affect older dogs.

The histologic and immunohistochemical findings along with the pattern of spread were most consistent with a PNET, although other findings that would have strengthened the conclusion, such as neuroblastic pseudorosettes and pseudopallisading cells, were not seen. Primitive neuroectodermal tumours are a group of malignant embryologic tumours derived from neuroepithelial cells. They have the potential to differentiate along a number of cell lines, sometimes within the same tumour, resulting in the complex histopathologic appearance seen in this dog.[31] Primitive neuroectodermal tumours may have a variable expression of GFAP, depending upon the level of glial differentiation, with some GFAP-positive reports in the dog.[32] Such variability makes reliable diagnosis of PNET challenging.[32] These tumours are very rare but have been reported in young dogs in the brainstem and cerebrum and in one case, in association with sudden death, consistent with the outcome in the dog of our report.[32-34] Both the MRI and CT features of PNET are variable. A tendency to disseminate along the CSF pathways has been described, however mineralisation has not been reported in animals and is uncommon in people.[6,35-37]

This report reinforces the need to consider multifocal congenital neoplastic conditions in young dogs presenting with seizures or clinical signs consistent with involvement of multiple neuroanatomic locations. Computed tomography is useful in assessment of mineralisation within the central nervous system, and as an easily performed, minimally invasive modality for identification of an intracranial mass effect in a animal with seizures. This case report also illustrates the complex and unpredictable nature of juvenile central nervous system neoplasia, the diagnosis of which is frequently controversial. As advanced MRI technology such as diffusion weighted and molecular imaging becomes more accessible to veterinary radiologists, antemortem diagnosis of brain tumours may become more sensitive and specific. Additionally, as our access to multi-panel immunohistochemical staining also expands, our understanding

of the behavior of primitive tumours of the juvenile central nervous system will advance.

ACKNOWLEDGEMENTS

The authors acknowledge Dr Sandy Adsett's contribution to the post-mortem examination and the initial pathology assessment.

REFERENCES

1. Chrisman CL Seizures. In Ettinger SJ and Feldman EC, editors. *Textbook of veterinary internal medicine – diseases of the dog and cat.* 4th edn Volume I. WB Saunders Company, Philadelphia 1995:152.
2. Poussaint TY. Magnetic resonance imaging of pediatric brain tumors: state of the art. *Top Magn Reson Imaging* 2001:6:411–433.
3. Wisner ER, Dickinson PJ, Higgins RJ. Magnetic resonance imaging features of canine intracranial neoplasia. *Vet Radiol Ultrasound* 2011:9:52:Suppl:52–61.
4. Koch MW, Sanchez MD, Long S. Multifocal Oligodendroglioma in three dogs. *J Am Anim Hosp* 2011:47:5:77–85.
5. Gonçalves R, Johnston P, Wessmann A, Penderis J. Imaging diagnosis-canine meningioangiomatosis. *Vet Radiol Ultrasound*. 2010:51:2:148-151.
6. Snyder JM, Shofer FS, Winkle TJ, Massicotte C. Canine intracranial primary neoplasia: 173 cases (1986–2003). *J Vet Intern Med* 2008;20:3:669–675.
7. Young BD, Levine JM, Porter BF, Chen-Allen AV, Rossmeisl JH, Platt SR. Magnetic resonance imaging features of intracranial astrocytomas and oligodendrogliomas in dogs. *Vet Radiol Ultrasound* 2010:52:2:132–141.
8. Motta L, Mandara MT, Skerritt GC. Canine and feline intracranial meningiomas: An updated review. *Vet J* 2012:192:2:153–165.
9. Kirmi O, Sheerin F, Patel N. Imaging of the meninges and the extra-axial spaces. *Semin Ultrasound CT MR* 2009:30:565-593.
10. Chamberlain MC, Sandy AD, Press G. Leptomeningeal metastasis. *Neurology* 1990:40:3:1:435-438.
11. Meltzer CC, Fukui MB, Kanai E, Smirniotopolous JG. MR imaging of the meninges. *Radiology* 1996:201:297-308.
12. Keenihan EK, Summers BA, David FH, Lamb CR. Canine meningeal disease: associations between magnetic resonance imaging signs and histologic diagnosis. *Vet Radiol Ultrasound* 2013:54:5:504-515.
13. Wang Y, Zou L, Gao B. Intracranial germinoma: clinical and MRI findings in 56 patients. *Childs Nerv Syst* 2010:26:12:1773–1777.
14. Brooks AN, Brooks KN, Oglesbee MJ. A suprasellar germ cell tumor in a 16-month-old Wagyu heifer calf. *J Vet Diagn Invest* 2012:24:3:587–590.
15. Patterson-Kane JC, Schulman FY, Santiago N, Mckinney L, Davis CJ. Mixed germ cell tumor in the eye of a dog. *Vet Pathol* 2001:1:38:6:712–714.
16. Plaza MJ, Borja MJ, Altman N, Saigal G. Conventional and advanced MRI features of pediatric intracranial tumors: posterior fossa and suprasellar tumors. *Am J Roentgenol* 2013:200:5:1115–1124.
17. Nagata T, Nakayama H, Uchida K, et al. Two cases of feline malignant craniopharyngioma. *Vet Pathol* 2005:42:5:663–665.
18. Spiess BM, Wilcock BP. Glioma of the optic nerve with intraocular and intracranial involvement in a dog. *J Comp Pathol* 1987:97:1:79–184.
19. Hoffman HJ, Humphreys RP Optic nerve glioma. In Lyons K, editor. *Tumors of the pediatric central nervous system.* Thieme New York 2001:302-304.
20. Eckersley GN, Geel JK, Kriek NP. A craniopharyngioma in a seven-year-old dog. *J S Afr Vet Assoc* 1991:62:2:65–67.
21. Nyska A, Harmelin A, Baneth G, et al. Suprasellar differentiated germ cell tumor in a male dog. *J Vet Diagn Invest* 1993:1:5:3:462–467.
22. Karavitaki N. Craniopharyngiomas. *Endocr Rev* 2006:27:4:371–397.
23. Mamom T, Meyer-Lindenberg A, Hewicker-Trautwein M, Baumgartner W. Oligodendroglioma in the cervical spinal cord of a dog. *Vet Pathol* 2004:41:5:524–526.
24. Armao D M, Stone J, Castillo M, et al. Diffuse leptomeningeal oligodendrogliomatosis: radiologic/pathologic correlation. *Am J Neuroradiol* 2000: 21:6:1122-1126.
25. Bishop TM, Morrison J, Summers BA, Delahunta A, Schatzberg SJ. Meningioangiomatosis in young dogs: a case series and literature review. *J Vet Intern Med* 2004:18:4:522–528.
26. Triolo AJ, Howard MO, Miles KG. Oligodendroglioma in a 15-month-old dog. *J Am Vet Med Assoc* 1994:205:986-988.
27. Ide T, Uchida K, Kikuta F, Suzuki K & Nakayama H. Immunohistochemical characterization of canine neuroepithelial tumors. *Vet Pathol* 2010:47:741-750.
28. Koestner A, Bilzer T, Fatzer R, Schulman FY, Summers BA, van Winkle TJ. *Histological classification of tumors of nervous system of domestic animals.* American Registry of Pathology, 1999.
29. Ferreira AJA. Mixed germ cell tumour in the spinal cord of a young dog. *J Small Anim Pract* 2003:44:81-84.
30. Valentine BA, Summers BA, de Lahunta A, White CL 3rd, Kuhajda FP. Suprasellar germ cell tumors in the dog: a report of five cases and review of the literature. *Acta Neuropathol* 1998:76:94-100.
31. Lantos PL, Vandenberg SR, Kleihnes P. Tumors of the central nervous system. In Graham D and Lantos PL, editors. *Greenfields Neuropathology*. 6th edn Volume II. Arnold, London 1997:700-710.
32. Headley SA, Koljonen M, Gomes LA, Sukura A. Central Primitive Neuroectodermal Tumour with ependymal differentiation in a dog. *J Comp Pathol* 2009:140:1:80–83.
33. Katayama KI, Kuroki K, Uchida K, et al. A case of canine primitive neuroectodermal tumor (PNET). *J Vet Med Sci* 2001:63:1:103.

34. Choi US, Philippe L, Alleman AR, Kim MS, Lee KC. Cytologic and immunohistochemical characterization of a primitive neuroectodermal tumor in the brain of a dog. *Vet Clin Pathol* 2012:41:1:153-157.

35. Turrel JM, Fike JR, LeCouteur RA, et al. Computed tomographic characteristics of primary brain tumors in 50 dogs. *J Am Vet Med Assoc* 1986;188:851–856.

36. Dick EA, Hugh MC, Kimberb C, Michalskic A. Imaging of non-central nervous system primitive neuroectodermal tumours: diagnostic features and correlation with outcome. *Clin Radiol* 2001:56:3:206-215.

37. Figueroa RE, Gamma TE, Brooks BS. Holgate RM, Miller R, William MR Findings on primitive neuroectodermal tumors. *J Comput Assist Tomogr* 1989;13(5):773-778.